

A physically-based model for the simulation of reactive turbulent objects

Arash HABIBI, Annie LUCIANI, Alexis VAPILLON

ACROE & CLIPS-IMAG

46 avenue Félix Viallet

38 031 Grenoble cedex FRANCE

Tel : (+33) 76 57 46 69 Fax : (+33) 76 57 46 02

Arash.Habibi@imag.fr, Annie.Luciani@imag.fr

Abstract

The challenging issue that is addressed here is the modelling of turbulent phenomena, physically consistent, and reactive at the same time. The aim is, first, to understand these phenomena in order to elaborate a particle-based dynamic model, capable of accounting for a certain number of experimentally observed recognizable turbulent phenomena (consistency). Next, the aim is to achieve not only beautiful shapes, not only the fine dynamics slow and fleeting, of turbulent objects left to themselves, but the still richer movements that result from the interaction with man. (reactivity).

This work presents a consistent connection with fundamental physics. However, it falls clearly in the field of computer graphics. We regard reactivity as a means to control a physically-based simulation of turbulent phenomena. We have elaborated several particle-based dynamic models which produce the target phenomena. Thanks to particles, we have simulated the interaction (action and reaction) between several fluids as well as between fluids and solid objects (fixed or mobile, rigid or deformable). When moved by an operator, these objects enable him to wave a hand in the fluid, to guide it, or to manipulate a thurible.

Eventually this coarse particle model is refined by a high-resolution dynamic model that adds the small-scale phenomena in the final animation.

Keywords : Turbulences, reactivity, physically-based, particles, refinement.

1. Introduction

1.1. Reactivity

The *reactivity* of a model is the extent to which it may react consistently to external actions occurring during the animation (for example obstacles, draughts etc.)

We evaluate the reactivity of a model by three criteria : reaction consistency, feedback and cost. *Reaction consistency* is the importance of the perceived causal relation between an action and the resulting observed deformations. It requires at least partial dynamic simulation.

Feedback is the extent to which the fluid may, in turn, act on the incident objects. Clearly, feedback requires a closed-loop system. Therefore it is totally impossible with kinematic models. In practice, again at least partial dynamic simulation is necessary. But it is not sufficient. In field representations, interaction (action and reaction) between separate independant objects cannot be taken in account by one field, but by as many fields as separate objects. The use of particle representation makes it possible to avoid this problem.

1.2. Large-scale models

Despite the great number of works on this subject, all of the current models seem to share a common structure, even though the elements of this structure are not identical. All comprise an *ambient* fluid, and an *incident* visible object (possibly particles or another fluid) carried by the ambient fluid. The former is typically modelled by a velocity or a force field, whereas the latter is modelled by particles.

In most cases, the global system is an open-loop, i.e. the actions are exerted by the ambient fluid on the incident particles without any possible feedback. First, the particles may be mere

tracers, i.e. follow a velocity field ([SF 93], [SF 95]) In this case, the only way to model or deform the fluid is to change the velocity field. Next, the particles may be placed in a force field and be dynamically simulated ([PP 94] [WH 91]). This results in a higher degree of consistency and feedback. However, in both cases, animation control and obstacle modelling are currently performed by changing the field.

In [CMTM 94] and [Gamito 95], the fluid↔particle system is a closed-loop system. In [CMTM 94], the flame (the velocity of the ambient fluid) can be deformed by an obstacle defined by physical properties and not by flow primitives.

For feedback, dynamic simulation and particles are both necessary ([MP 89], [LJRCF 91]).

In this work, our major aim is reactivity (consistency, feedback, low cost) Therefore, the ambient fluid and the incident fluid, as well as all sorts of obstacles and solid objects (rigid or deformable) are dynamically simulated at the same level, with the same particle system *Cordis-Anima* [LJCFR 91] (Appendix). Thanks to this formalism, any type of object, moved kinematically or dynamically, may act as an obstacle, create a draught, guide the flow, or be the support of the fluid source. These objects may be handled by a human operator, they enable him to blow on the curls, to put a hand in them or to manipulate a thurible. In all cases, the behaviour of the fluid remains physically consistent.

1.3. Small-scale phenomena

There are several methods to add small-scale details to the large-scale models mentioned above. This “refinement” operation may be applied on the velocity field or on the particles. [SF 93] and [SF 95] refine the velocity field by adding a filtered spatial white noise to the large-scale velocity field. For particles, modelling the small-scale, or mere visualization, requires that each particle be associated with a continuous shape or a finer distribution. These shapes or distributions will eventually combine in order to make the global shape of the object.

In [Ina 90], this shape is time-independent and spherical. In [SF 93], the size of the shape is time-dependent (modelling diffusion and dissipation) but it remains spherical. In [PP 94], each particle is associated with a Gouraud-shaded regular hexagon. The shape of these particles changes according to an explicitly time-dependent law. The shape of the particles may also change according to its movement in the course of time. In [CMTM 94] and in [PP 94], each particle leaves on the final image, a trace that represents its successive positions in the course of time. This is the “long exposure” method. Another type of more complex time integration is performed in [SF 95]. The shape of the particle depends not only on the movement of the particle, but it varies according to the value of the velocity field at the underlying points. This is called “time warping”, and it produces very fine and realistic wisps of smoke.

We need a generic model that be coherent, both with the underlying small-scale phenomena (dissipation, flow) and with the movement of the particles. Therefore we elaborated a physical model, which furthermore is excited by the particles of the large-scale model. In addition, we use a field representation for the small-scale model, since the model is linear but necessarily high-resolution.

1.4. Minimal models

Reactivity and interaction with man requires high simulation rates. This is why we need minimal models, i.e. models such that the slightest simplification would result in an inconsistent model. However, since for reaction consistency and feedback, dynamic simulation is necessary, we will limit our research to minimal dynamic models.

A model is said to be consistent with respect to a set of recognizable criterion-phenomena if and only if, it is capable of producing them. Our criterion-phenomena comprise plain curls, Kelvin-Helmholtz eddies and Von Karman vortex streets [Les 94]. Our research procedure consists of starting from the simplest fluid models. If none of the target phenomena are observed we successively add different characteristics to the model, until at least one of the phenomena (Φ) is observed. Then we try to simplify this model. We continue the simplification process until the resulting model can still produce the criterion phenomena, but could not produce them if it were simplified in any way (less complex interactions, fewer particles, fewer interactions etc) .

This final model is the minimal dynamic model associated with phenomenon Φ , and it contains the necessary and sufficient conditions in which Φ can be observed (i.e. the causes of Φ). In

the next steps, we add more characteristics in order to find the minimal models of the more complex target phenomena.

Section 2 describes our experiments and the various resulting minimal models. Section 3 presents the results of reactivity tests on the previous models. Section 4 is a presentation of our small-scale refinement model, and section 5 presents conclusion and future work.

2. The search of minimal macroscopic models

2.1. Viscosity

2.1.1. The mixing layer

Let there be a fluid divided in two zones with different convection velocities (figure 1) The junction between these zones is a layer of high velocity gradient and is called the *mixing layer*. Most turbulences occur in this unstable layer. At the slightest perturbation, a steady laminar flow turns into a set of eddies and whirlpools. In the following, our aim is to model the behaviour of this layer.

2.1.2. Viscous particle model

In a first step, our aim is to find out the major phenomena that can be produced by purely viscous models : Two adjoining elementary blocks of fluid in viscous interaction define a macroscopic model of a viscous fluid. If we neglect the rotation and deformation degrees of freedom for the elementary blocks, each can be modelled by a punctual mass with three translation degrees of freedom. The resulting model is a set of punctual masses linked by viscous interactions. Each particle does not represent a molecule but a block of fluid whose size is a parameter.

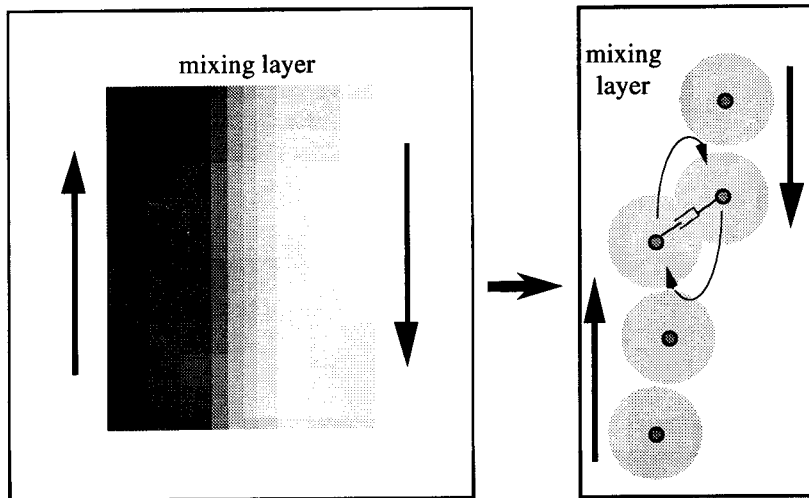


figure 1. At a macroscopic scale (left) dynamic viscosity accounts for molecular collisions in the mixing layer. We modelled this by punctual masses linked by thresholded viscous interactions (right)

2.1.3. curls

To evaluate this model, we carry out a series of experiments, in which we reproduce the conditions of the mixing layer, i.e. two fluids with different convection velocities. The fluids are modelled by particles.

In order to obtain a very minimal model, in a first step, we model one of the fluids by a grid of masses linked together by linear visco-elastic springs (Appendix). If the interaction between the two fluids are only linear viscous interactions, no curls are observed. In order to account for the rotation phenomena in the fluid's mixing layer, we add one characteristic to the previous model, and that is the use of a non-linear viscous interaction called the *thresholded viscous* interaction (Appendix). The resulting behaviour is : curls, heaps, and fractures, with dissipation.

2.1.4. Kelvin-Helmholtz eddies

The previous model in which one of the fluids had a very constrained movement is not general enough to produce other typical profiles of turbulent phenomena such as Kelvin-Helmholtz eddies. A much more general model of the Newton's third law is composed of two sets of free particles, all in thresholded viscous interaction.

When the flow of both jets has reached a steady laminar regime, we introduce a perturbation such as a shock, by means of a colliding small mass which pushes the lower jet on the upper jet. Figure 2 shows the resulting properly formed Kelvin-Helmholtz whirlpools. In the beginning, the outer layers are still in laminar flow, but eventually, they too get involved in the whirlpool.

As a conclusion, viscosity is sufficient for the achievement of Kelvin-Helmholtz turbulences. This results validates the bases of our fluid model. However, for other phenomena such as dissipation and for another chief figure of turbulent fluids, i.e. Von Karman vortex streets, the viscous model is not sufficient.

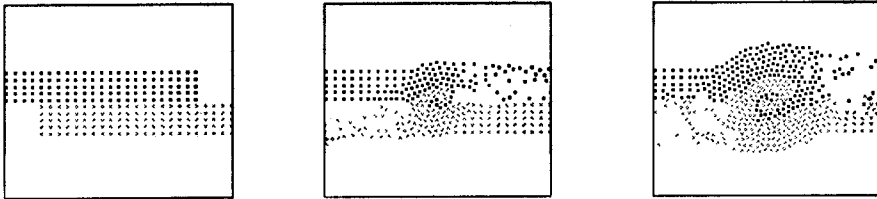


figure 2. Multi-layer whirlpool. The time step of this chronogram is 6 sec

2.2. Pressure

2.2.1. Von Karman vortex streets

This is a complex figure, composed of several Kelvin-Helmholtz whirlpools. It occurs when there is frontal shock in the fluid. It occurs typically behind obstacles placed in a uniform flow, or in a jet introduced in another fluid environment, (cigarette smoke for example). It is composed of one major oscillation, due to the depression after the obstacle, and small Kelvin-Helmholtz eddies at each period, due to the fact that after the obstacle there are two zones : one low-velocity zone right behind the obstacle and two high velocity zones on both sides. This creates two interfaces, and therefore two mixing layers with opposite torques.

2.2.2. The elastic particle model

The previous viscous model is the discretization of a Newtonian fluid verifying the Navier-Stokes equation without pressure. In this section, we will add pressure to our model. Like viscosity, pressure is also an emergent phenomenon, due to the integration of molecular collisions in the direction of the flow. In our models, a particle represents an elementary block of fluid. We approximate pressure by adding between each particle and all the other particles, a *thresholded elastic* interaction (also called *elastic buffer* interaction. Cf Appendix) It all happens as if every particle had a spherical repulsion zone around it. We used high values for d_{e0} and low values for the stiffness k . (These parameters are defined in the appendix) .In this way the repulsion zones of a great number of particles superimpose and the repulsion forces are added, which causes local pressure.

The introduction of a repulsion force requires a confined system. Such a confinement can be modelled by setting a visco-elastic buffer interaction with external masses acting as walls. This interaction must not be too stiff, in order to avoid the occurrence of shock waves from the walls. Instead of rigid walls, fairly loose elastic buffer interactions enable us to model external pressure.

3. Results

If one of the jets is replaced by a set of particles scattered over the simulation space we obtain the major effects that appear in a fluid flowing in a medium. Figure 8 shows Von Karman profiles with inversed Kelvin-Helmholtz eddies.

Thus smoke behaviour has been modelled, including all the phenomena mentioned above : laminar flow, whirlpools, Von Karman vortex streets, dissipation.

Typically our final simulations were carried out with $d_{e0}=9$ cm and $k=0.15$ N/m, whereas in the same model, for the thresholded viscous interaction we use $d_{v0}=3.5$ cm and $z=5.0$ N/m.s⁻¹. These parameters are defined in the appendix.

Furthermore, the mass of our particles is $m=0.05$ kg. All of our simulations are carried out with a time step of $T_e = 1/1050$ seconds.

3.1. Obstacles

We model obstacles as particles in visco-elastic buffer-type interaction with the fluid particles. The difference between this model with a simple repulsion force field can be seen in the expression of the buffer interaction (appendix) : the forces are exerted in both ways. The obstacles exert repulsion on the fluid particles, but the particles also exert forces on the obstacles. Therefore, the obstacle can be fixed but also moved, possibly by a human operator (figure 3) and even by the fluid itself as the leaves in [WH 91]. The simulation is closed-loop. An object assimilated to a leaf may rise in an ascending current and next fall down and, in turn, create turbulences in the ambient fluid.

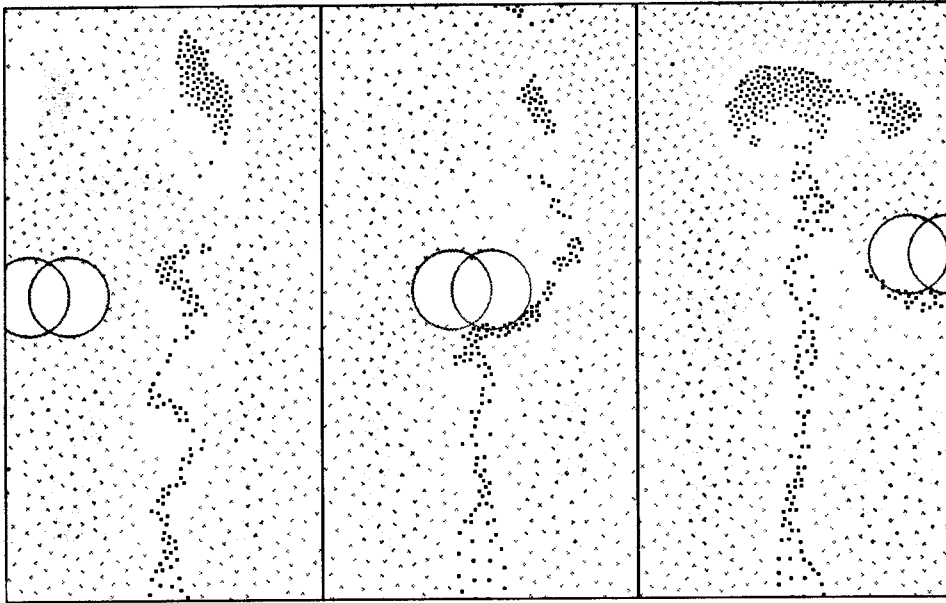


figure 3. A gesture guided object moving from the left to the right, interacting with the fluid

3.2. Particle sources

The fluid source is also a particle-object as any other. It can be placed on a fixed point (figure 3), on an object manipulated directly by a human operator (figure 4) or on any other object, possibly moving under the influence of the fluid. On figure 5, the source is placed on a thurible manipulated by a human operator. In this case also, the interactions are two-way interactions. A source emits particles, and, at the same time, undergoes a reaction force in the opposite direction of the jet.

4. Microscopic model - refinement

The microscopic model must take in account the properties of the small-scale phenomena such as flow, dissipation, diffusion etc, and insure dynamic coherence with the behaviour of the particles of the macroscopic model. This is why it must be a dynamic model. As we mentioned in § 1.2., the refinement of particles implies to associate each particle with an elementary volume that be likely to combine with other volumes to form the global shape.

In our case, in view of the high deformability of this type of material, this volume must be physically deformable. Because of the high resolutions required for these phenomena, and since they can be approximated by linear models, we have chosen a field representation.

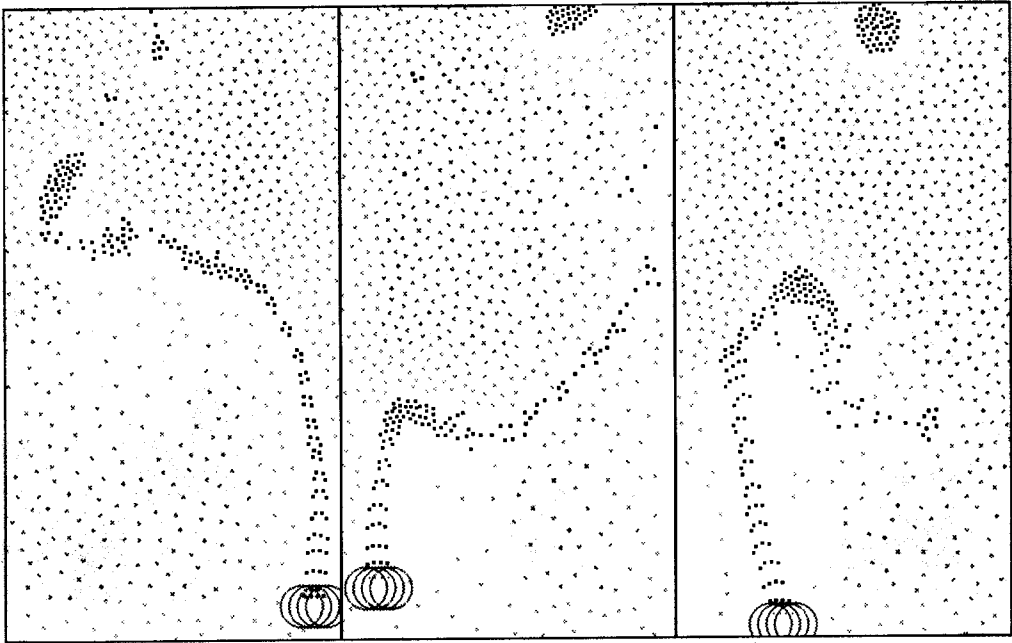


figure 4. The source is placed on an object manipulated by a human operator

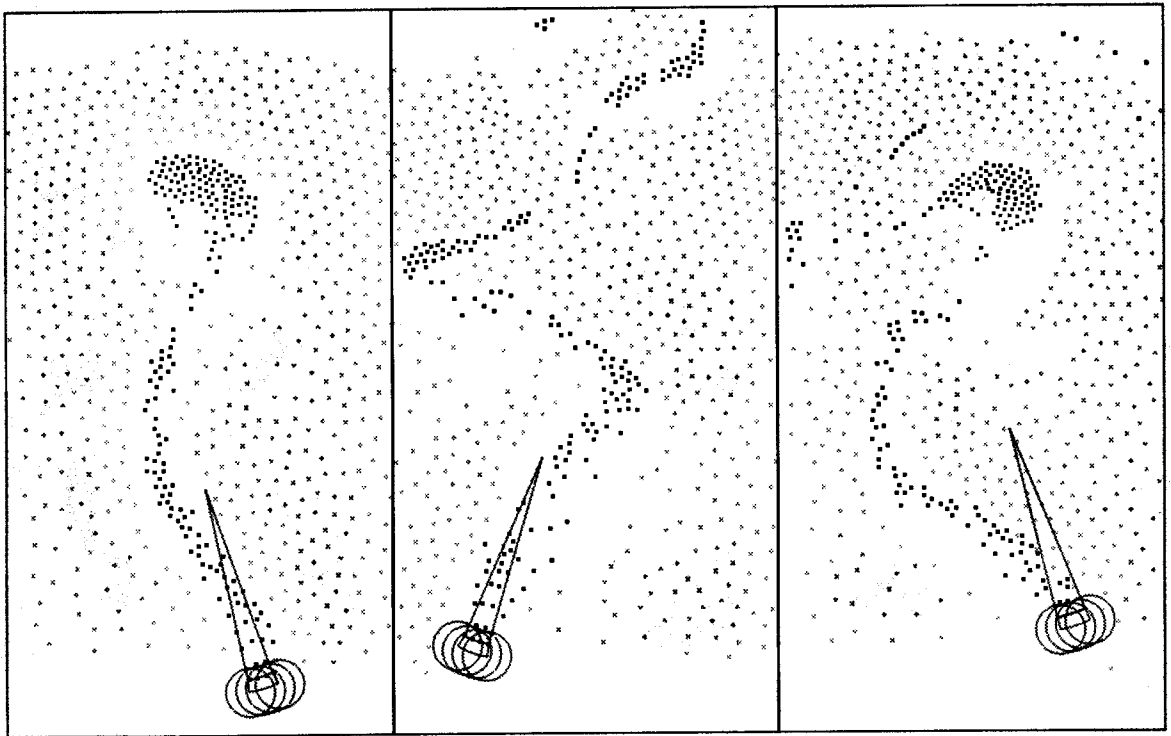


figure 5 The source is placed on a thurible also manipulated by a human operator

4.1. A physically deformable surface

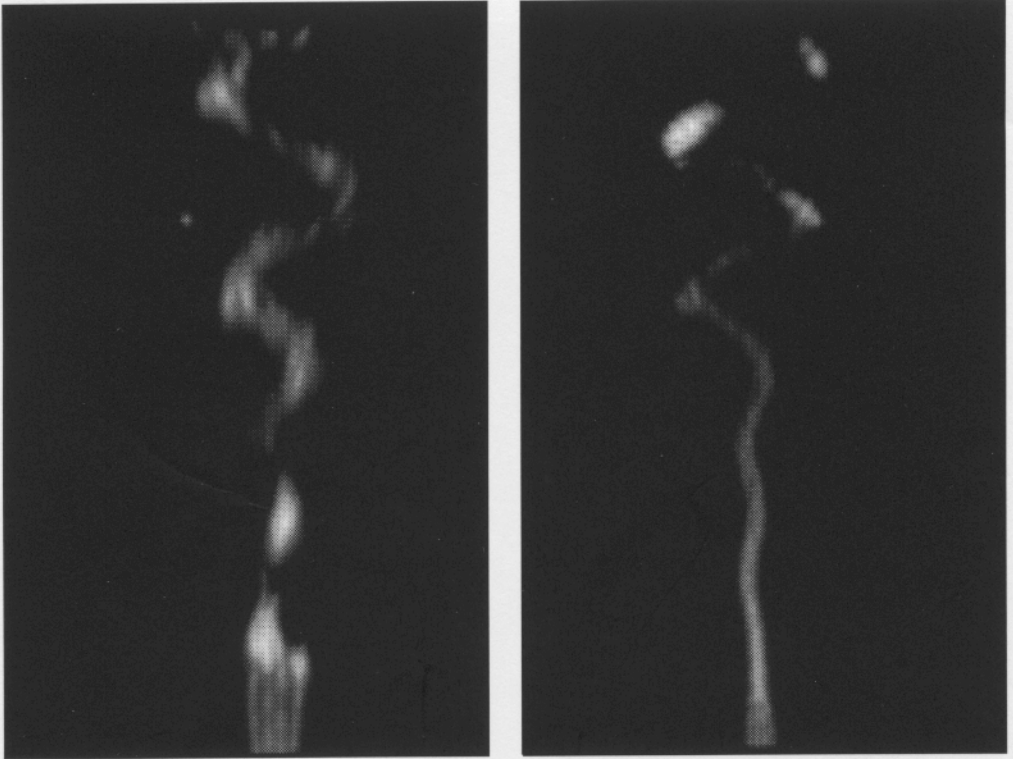
In field representation, each point in space must be characterized by a scalar which represents the amount of matter present in the vicinity of that point, or in other words the "presence field". Of course, given the macroscopic model studied in section 2, this presence depends greatly on the presence or not of particles in that vicinity. But this is not enough since the particles do not account for the small-scale phenomena.

This is why we simulate a deformable surface that covers the whole scene. When a particle passes over the surface, it causes deformation. We use the deformation field of this surface as the presence field which provides the value of the spatial occupation at that point. The small-scale phenomena are taken in account by the physical properties of this physical surface.

The final rendered image, is eventually directly obtained from the deformation field thanks to an oversampling. The light value is proportional to the value of the deformation. On figures 6, 7 and 8, the dark areas correspond to zones where the deformation is zero. Lighter zones correspond to high values of deformation, to zones deformed by a particle.

4.2. A discrete network of masses

This surface is a square-tesseled network whose nodes are punctual masses called *phyxels*. [LHM 95] All of them move perpendicularly to the scene. The deformation field at a given phyxel is the measured along this direction and it equals the difference between its current position and its rest position. This rest position is determined by linear visco-elastic interactions linking each phyxel to a rigid substratum. The propagation of the excitations is modelled by the same type of interactions between each phyxel and its four-neighbours. The proper excitation of the field by the macroscopic scale particles is modelled by visco-elastic buffer type interactions. Given this set of parameters, this deformable surface is characterized by a certain number of deformation modes. Each is characterized by a shape, a type (oscillating, damped, critical) and an amplitude.



figures 6 and 7. Two simulations of turbulent phenomena after refinement. The Von Karman vortex street can clearly be recognized on figure 7

The movement of the particles on this deformable surface excites differently its deformation modes. Depending on the value of the parameters of this network, the particles would either excite damped modes (as for sand and smoke) or oscillating modes (as for rain or liquid surfaces) The same set of parameters enables us to control the propagation of these excitations and even the length of the waves produced on the surface.

The area where the propagated deformation of a marking particle exceeds some small threshold ϵ , is the particle's *Zone of Influence* (ZI_ϵ). The zone of influence $ZI_\epsilon(P,t)$ of particle P is the time-dependant shape that we associate with each particle (Cf § 1.3). When most modes are damped, the zone of influence of a particle at rest is a circle with gradations and a blur. Dynamically, this final circle is not reached immediately. Ther particle exerts a first excitation which propagates more or less rapidly (depending on the stiffness of the higher order modes of the surface) and causes the zone of influence to expand in area but to decrease in amplitude. This accounts for dissipation. The ZI of a moving particle has also a light "comet's tail" whose size, direction and intensity distribution depend on the particle's velocity and trajectory. In

addition, for damped surfaces, this surface performs low-pass filtering. Therefore, for higher values of stiffness between phyxels, a group of close particles is visualized as a continuous stretch of matter (figures 6, 7 and 8).

5. Conclusions

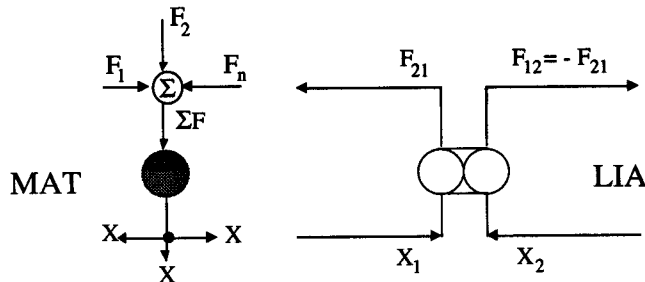
Our final particle model (section 2) : (1) is at a larger scale than the molecular scale and models emergent effects such as viscosity and pressure with punctual masses in interaction. (2) integrates cohesion forces (viscous forces) that cause eddies, and repulsion forces that cause superpressure and depression, that intensify confinement or the fluid's dispersion and that also cause shock wave propagation, (3) properly reproduces the major characteristic figures of turbulent fluids such as plain curls, Kelvin-Helmholtz eddies and Von Karman vortex streets. Moreover the obtained model is indeed reactive and minimal. These simulations were all carried out at 1050 Hz. With a non-optimized version of the physical modeller (i.e. with the complete calculation of $n(n-1)/2$ interactions for n masses) these simulations cost typically 2 seconds per sample on a Silicon Graphics Indigo workstation. This time can be divided by 2 on an Indigo 2 Extreme.

The refinement model is a finely discretized 1D linear $O(n)$ model. The final results are displayed on figures 6, 7 and 8. These refinement simulations, with 400 smoke particles and 57 600 phyxels, at the simulation frequency of 100Hz required 7.06 seconds per frame on a Silicon Graphics Indigo 2 Extreme workstation. However, this refinement model can easily be parallelized and implemented on a massively parallel machine.

Appendix

The *Cordis-Anima* physical modeller-simulator, based on point physics has already been described in many other papers [LJCFR 91]. However, in this appendix we will mention some major elements necessary for the comprehension of the algorithms described in this paper.

Cordis-Anima objects are networks composed of two types of automata : MAT and LIA. In these networks, all of the nodes are MAT automata (which represent the particles) These nodes may or may not be linked by arcs : LIA automata (which represent the physical interactions). Each MAT automaton can be connected to as many LIA elements as wished. Each LIA automaton can be connected to two MAT automata (one at each end).



MAT and LIA : the two basic atoms of the *Cordis-Anima* modeller-simulator



figure 8 The same situation as on figure 5 after the refinement

The networks described in this papers are characterized by an agglomerate topology, i.e. that each MAT automaton (particle) is linked to all the other MAT automata by LIA automata.

Now let us present the algorithm implemented in these automata.

One MAT automaton represents one particle. One such automaton reads a force F (the forces applied to the particle) and produce one position X (the position of the particle). For 1D masses F and X are scalars and for 3D masses they are vectors. The algorithm implemented in MAT automata is Newton's second law.

$$F = m \cdot \ddot{X} \Leftrightarrow X = \frac{1}{m} \iint F dt^2$$

Where m is the mass of the particle. LIA automata read two positions X_1 and X_2 (and/or two velocities) and produce two opposite forces F_{12} and F_{21} . The underlying algorithm is a piecewise linear function called the *interaction function*. In the following we present the expressions of the various interaction functions mentioned in the paper.

k represents stiffness of the interaction, z represents its viscosity. d_0 represents the rest length of the linear interaction, and d_{e0} and d_{v0} represent respectively the elastic and viscous thresholds.

A.1. Linear visco-elastic interaction

$$F_{12} = -F_{21} = \left(-z_0 \cdot \frac{\partial}{\partial t} |X_1 - X_2| - k_0 (|X_1 - X_2| - d_0) \right) \cdot u_{12}$$

$$\text{where } u_{12} = \frac{X_1 - X_2}{|X_1 - X_2|}$$

A.2. Thresholded elastic interaction

(buffer interaction)

$$\text{if } |X_1 - X_2| \geq d_{eC} \quad F_{12} = F_{21} = 0$$

$$\text{if } |X_1 - X_2| < d_{eC} \quad F_{12} = -F_{21} = -k_0 (|X_1 - X_2| - d_{e0}) \cdot u_{12}$$

A.3. Thresholded viscous interaction

$$\text{if } |X_1 - X_2| \geq d_{vC} \quad F_{12} = F_{21} = 0$$

$$\text{if } |X_1 - X_2| < d_{vC} \quad F_{12} = -F_{21} = -z_0 \cdot \frac{\partial}{\partial t} |X_1 - X_2| \cdot u_{12}$$

A.4. Thresholded visco-elastic interaction (visco-elastic buffer interaction)

This is equivalent to an elastic and a viscous interaction in parallel between the same two MAT automata.

References

[Gre 73] D. Greenspan *Discrete Models*, Reading in Applied Mathematics, Addison Wesley, 1973

[MP 89] G. Miller, A. Pearce *Globular Dynamics : A Connected Particle System For Animating Viscous Fluids*, Computer & Graphics Vol 13, No. 3, pp 305-309 1989

[LJCFR91] A. Luciani, S. Jimenez, C. Cadoz, J.L. Florens, O. Raoult *Computational Physics : a Modeler - Simulator for Animated Physical Objects*, Proceedings of Eurographics Conference, 1991, Vienna, Austria

[WH 91] J. Wejchert, D. Haumann *Animation Aerodynamics* In Proceedings of SIGGRAPH' 91 Volume 25, Number 4, July 1991

[CMTM 94] N. Chiba K. Muraoka H. Takahashi and M. Miura *Two-dimensional Visual Simulation of Flames, Smokes and the Spread of Fire*. The Journal of Visualization and computer Animation, vol 5, pp 37-53, 1994.

[GLG 95] M.N.Gamito P.F. Lopes M.R. Gomes *Two-dimensional simulation of gaseous phenomena using vortex particles* Computer Animation and Simulation '95 (Springer-Verlag Wien New York) pp 3-15

[PP 94] LC. H. Perry, R.W. Picard *Synthesizing Flames and their Spreading* Proceedings of the Fifth Eurographics Animation and Simulation Workshop (Oslo, Norway September 17-18 1994)

[SF 93] J. Stam and E. Fiume *Turbulent Wind Fields for Gaseous Phenomena* ACM Computer Graphics (SIGGRAPH' 93), p 369-376, August 1993

[SF 95] J. Stam and E. Fiume *Depicting Fire and Other Gaseous Phenomena Using Diffusion Processes* ACM Computer Graphics (SIGGRAPH' 95), p 129-136, August 1993

[INA 90] M. Inakage *A Simple Model of Flames* Proceedings of CG International'90, pp. 71-81

[LHM 95] A. Luciani, A. Habibi, E. Manzotti *A Multi-Scale Physical Model of Granular Materials* Proceedings of Graphics Interface' 95.

[CLF 93] C. Cadoz, A. Luciani, J.L. Florens *CORDIS-ANIMA A Modelling and Simulation System for Sound and Image Synthesis - The General Formalism*, Computer Music Journal, 1993, 10(1), 19-29, M.I.T. Press

[Les 94] M. Lesieur *La Turbulence* Presses Universitaires de Grenoble 1994